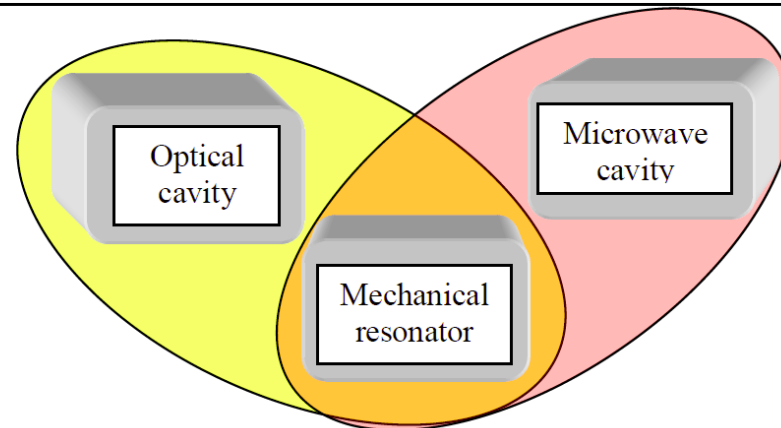


WP2 PHOTON-PHONON-INTERFACES

WP2: Photon-phonon interfaces

Main objective: implementation of coherent interconversion between microwave/optical photons and MHz/GHz phonons



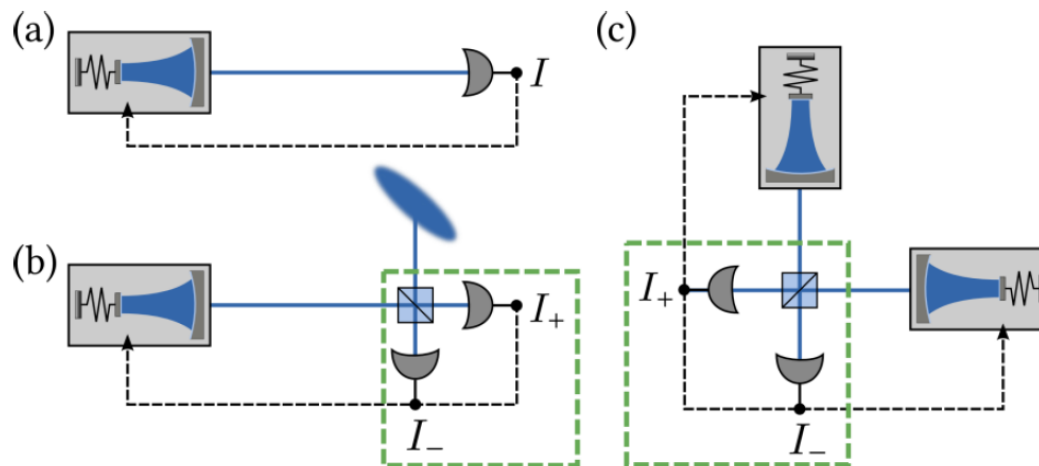
Deliverables:

- D2.3 Detection of optomechanical correlations by means of quantum filtering techniques (Month 24)
- D2.4 Coherent photon-phonon conversion in an optomechanical system (Month 24)
- D2.5 Demonstration of large single-photon optomechanical coupling rates (one order of magnitude improvement in g_0/κ) at cryogenic temperatures (Month 36)

D2.3 Detection of optomechanical correlations by means of quantum filtering techniques (Month 24)

LUH + UNIVIE:
design and analysis of novel quantum protocols
to control the mechanical system

- employ **optomechanical entanglement as a resource** for measurement-based feedback protocols:
 - preparation of a low-entropy mechanical state by feedback cooling
 - creation of bipartite mechanical entanglement by time-continuous entanglement swapping
 - preparation of a squeezed mechanical state by time-continuous teleportation.



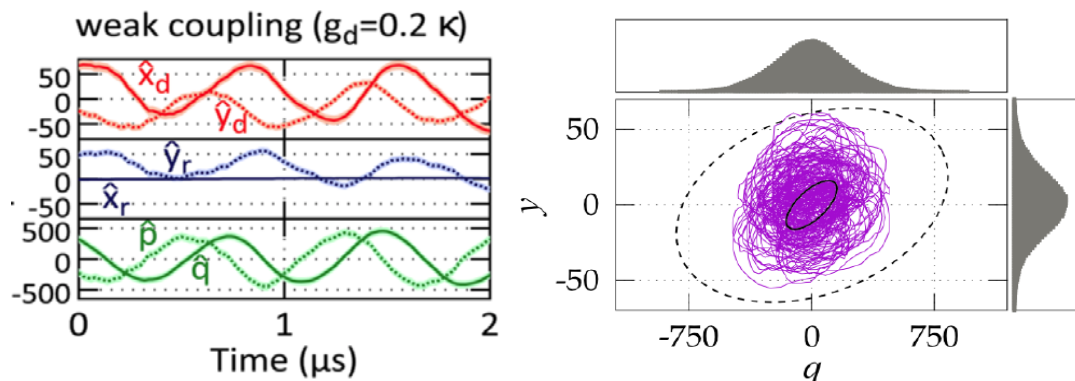
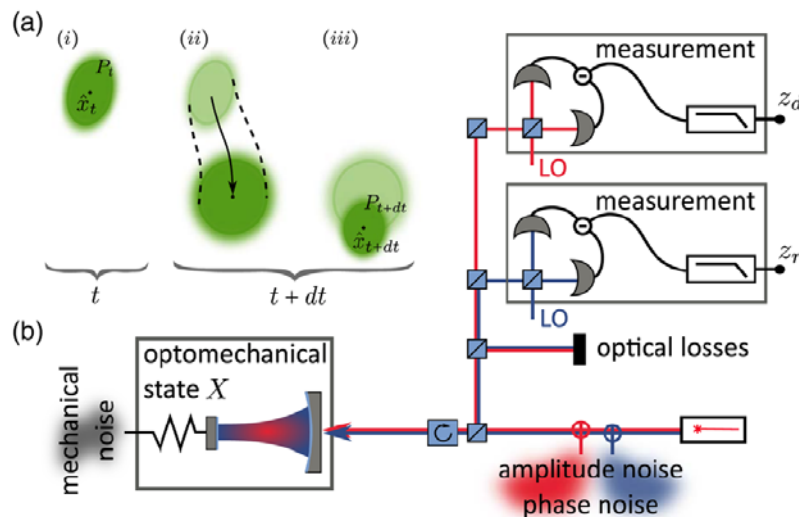
Physical Review A 91, 033822 (2015)

extensive toolbox for time-continuous
control of optomechanical systems

D2.3 Detection of optomechanical correlations by means of quantum filtering techniques (Month 24)

UNIVIE + LUH:
observe optomechanical correlations using
Kalman filtering

- based on accurate model of experimental setup (including colored laser amplitude and phase noise, photon losses, multiple mechanical modes)
- produces the least-square-error estimates of optomechanical dynamical variables
- trajectories allow monitoring of optomechanical correlations in real time



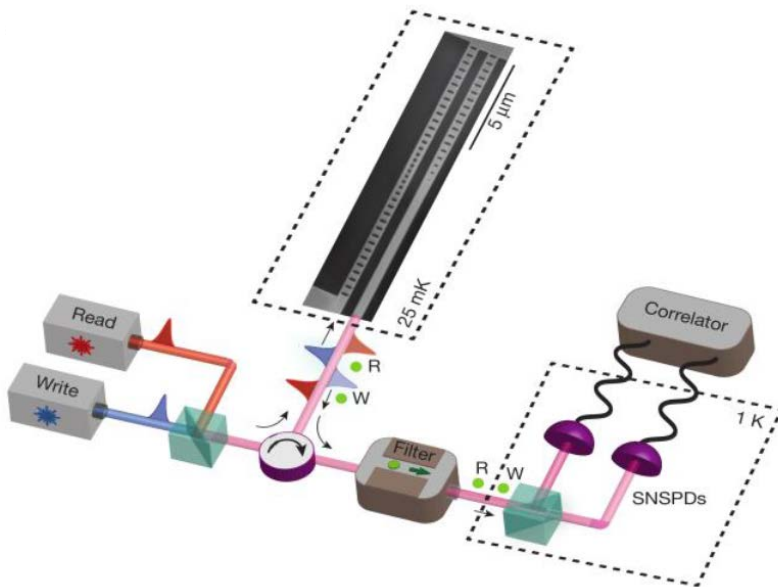
towards real-time optimal (classical and quantum) control of cavity optomechanical systems

D2.4 Coherent photon-phonon conversion in an optomechanical system (Month 24)

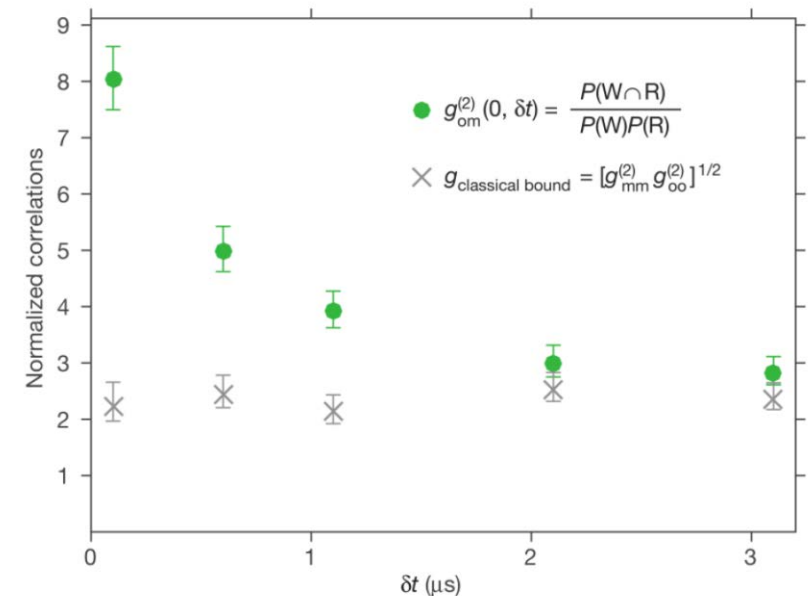
UNIVIE + TU Delft:
coherent **photon—phonon—photon**
conversion on the level of single quanta

fully quantum protocol:

- initialization of the resonator in its quantum ground state of motion
- subsequent generation and read-out of *correlated photon—phonon pairs*
- violation of Cauchy-Schwarz inequality:
- unambiguous evidence for non-classical mechanical state



on-chip solid-state mechanical resonators as
light–matter quantum interface



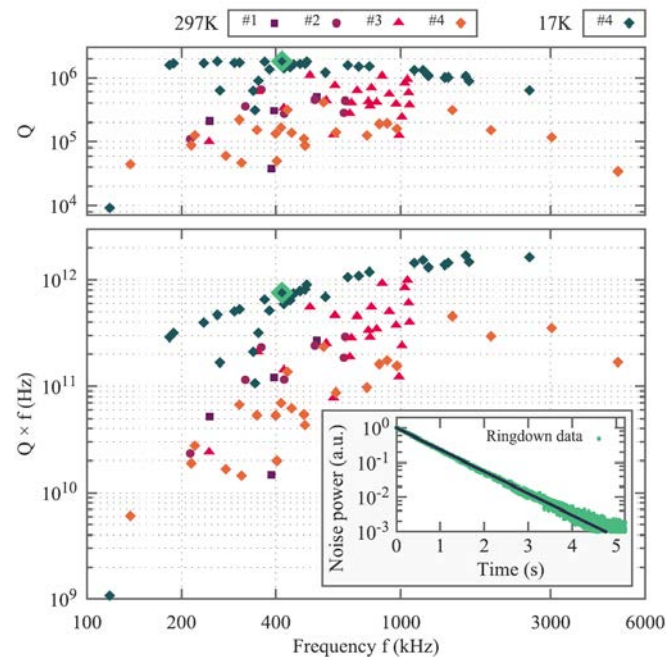
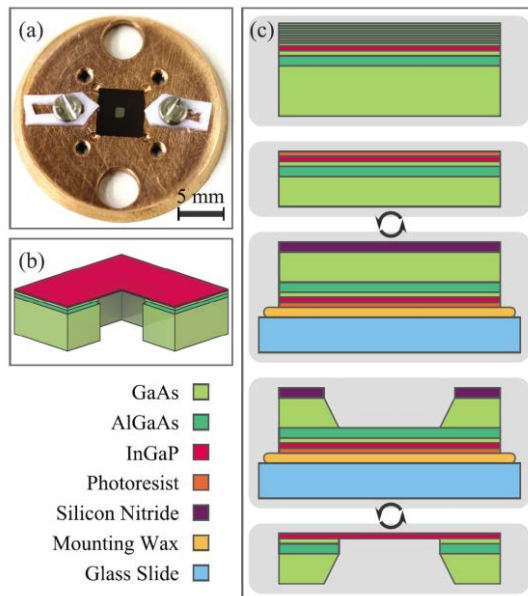
Nature 530, 313 (2016)

D2.5 Demonstration of large single-photon optomechanical coupling rates (one order of magnitude improvement in g_0/κ) at cryogenic temperatures (Month 36)

UNIVIE + JILA:
optomechanical properties of tensile-strained
 $\text{In}_x\text{Ga}_{1-x}\text{P}$ nanomembranes on GaAs

intrinsic tensile strain to a monocrystalline thin film of $\text{In}_x\text{Ga}_{1-x}\text{P}$

- mechanical quality factors of $>10^6$
- Q-f products of $>10^{12}$
- optical loss <40 ppm@1064nm



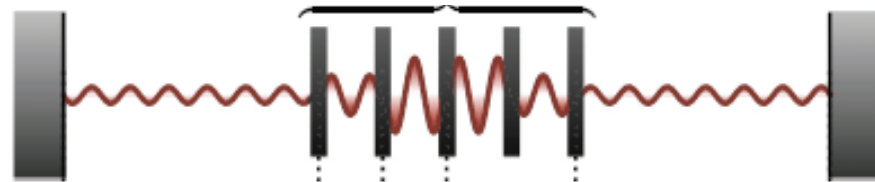
novel experimental architecture for realizing **stacks of membranes** for enhanced optomechanical coupling

Applied Physics Letters 104,
201908 (2014)

LARGE SINGLE-PHOTON COUPLING WITH **TWO** MEMBRANES-IN-THE-MIDDLE

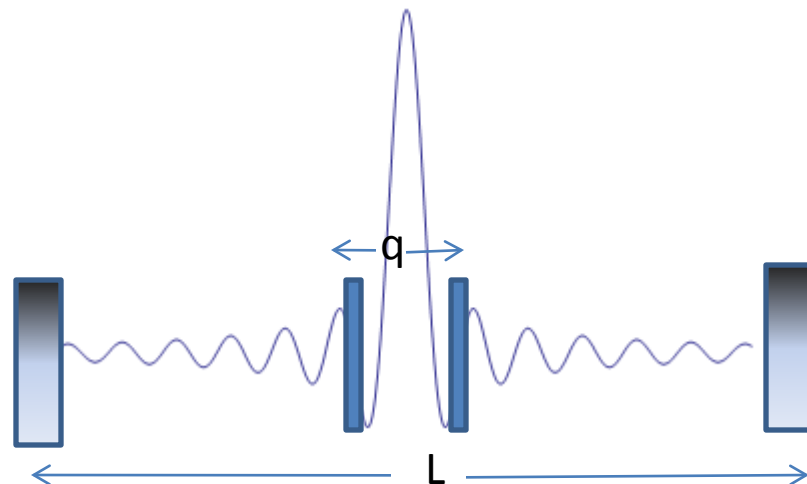
Strong optomechanical coupling can be achieved with a stack on N equidistant membranes in a Bragg reflector configuration

Strong coupling is obtained when light is mostly confined within the membranes

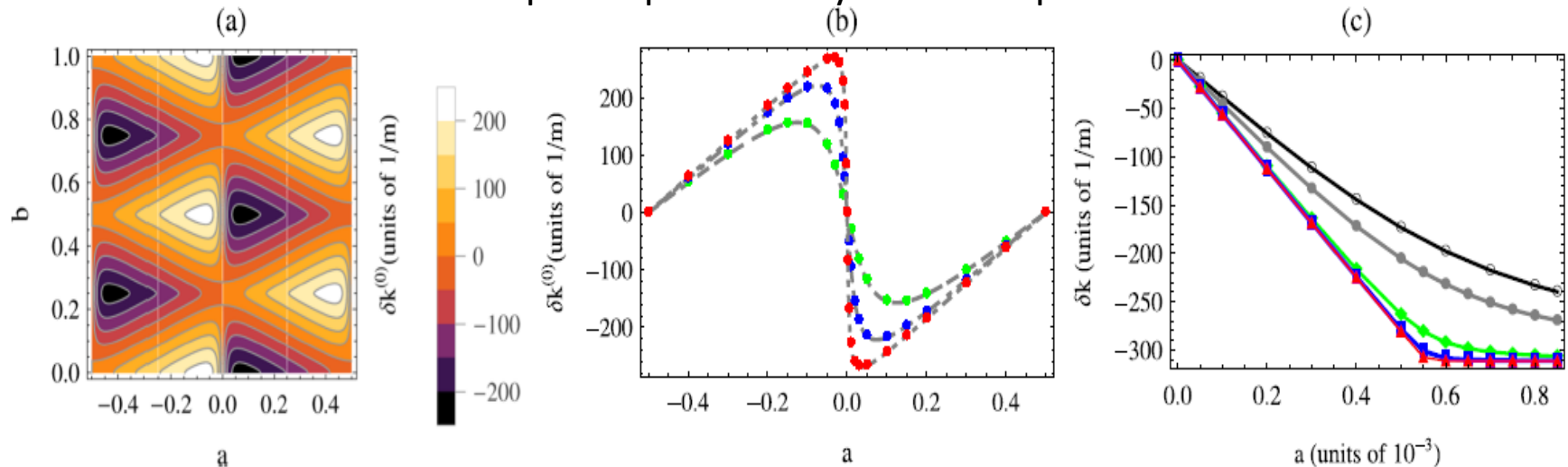


We have shown (J. Li et al, J. Opt. 2016) that the strong coupling condition can be achieved already with TWO membranes only

$$\frac{g}{\kappa} \approx 1$$



From the explicit optical cavity mode frequencies



(a) Frequency shift of a cavity mode as a function of membrane distance $q = (10.5+a) \lambda$ and their center of mass $Q=b\lambda$, for $R_m = 0.8$. (b) Frequency shift versus $q = (10.5+a) \lambda$ ($Q = 0$), for various values of the reflectivity: $R_m = 0.5$ (dashed curve; green dots), $R_m = 0.8$ (dotted-dashed; blue dots) and $R_m = 0.95$ (dotted; red dots). (c) The same as (b), very close to the limit $R_m = 1$. In practice we take $T_m = 1 - R_m = 2 \times 10^{-3}$, (black); 10^{-3} (gray); 10^{-4} (green); 10^{-5} (blue); 10^{-6} (red).

We find for the relative motion optomechanical coupling

$$g_q = -\frac{\cos(2k^{(0)}Q) + \sqrt{R_m}}{T_m} g_{\text{sing}}$$

which saturates for $R_m \rightarrow 1$, to

$$\frac{\omega_0}{q} x_{\text{zpm}} = g_q^{\text{max}},$$

Strong coupling is achieved for membrane reflectivities $R_m \rightarrow 1$ and when the inner cavity is close to resonance

- The ratio g/k is significantly improved because the the coupling tends to that of the inner cavity, while the finesse remains that of the external, longer cavity.

$$\left| \frac{(g/\kappa)_{\text{double}}}{(g/\kappa)_{\text{sing}}} \right| = \left| \frac{g_q^{\text{max}}}{g_{\text{sing}}} \right| = \frac{L}{2q}$$

The price to pay is that the membrane separation and alignment has to be controlled at the level of $\lambda (1-R_m)$

Qubit coupled to resonator

► Qubit

► photonic cavity

$$H_c = \omega_c \left(\hat{a}^\dagger \hat{a} + \frac{1}{2} \right)$$

► phononic cavity

$$H_m = \omega_m \left(\hat{b}^\dagger \hat{b} + \frac{1}{2} \right)$$

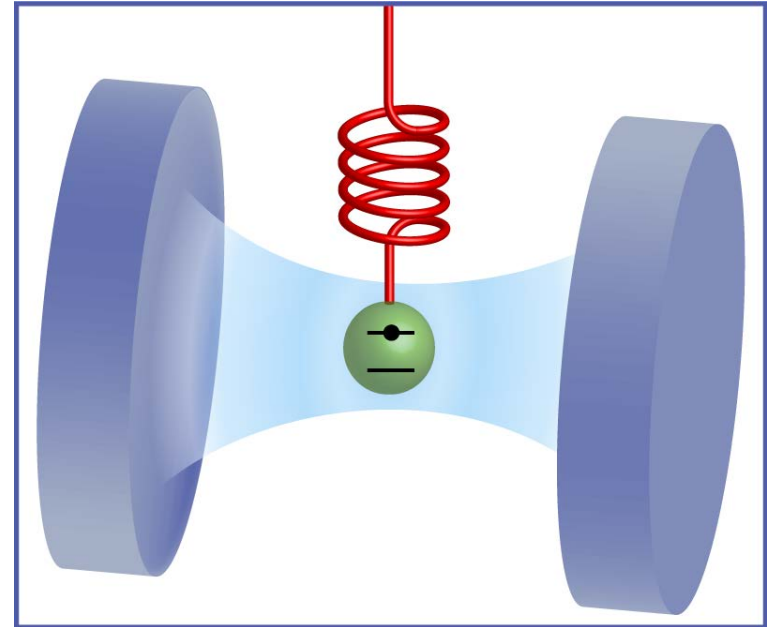
$$H = H_{\text{QB}} + H_c + H_m + H_{\text{QB-c}} + H_{\text{QB-m}}$$

$$H_{\text{QB-c}} = g_c (\hat{a}^\dagger + \hat{a}) \hat{\sigma}_x$$

$$g_m \approx 100 \text{ MHz} \approx f_m$$

$$H_{\text{QB-m}} = g_m (\hat{b}^\dagger + \hat{b}) \hat{\sigma}_z$$

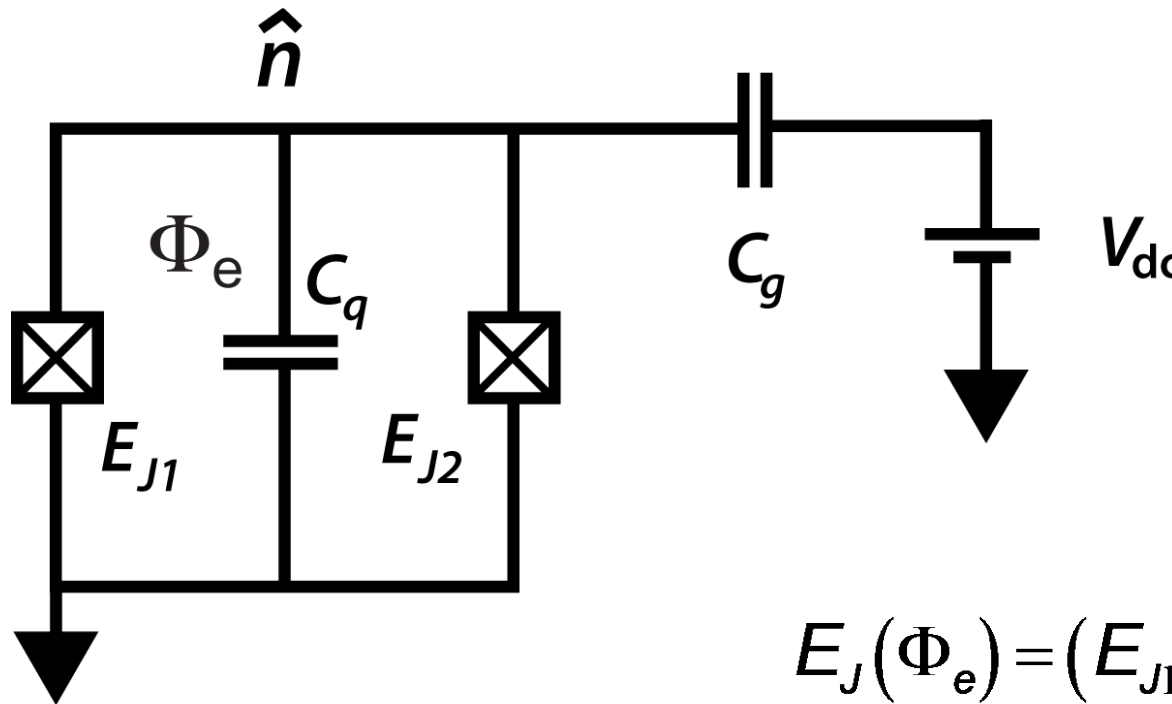
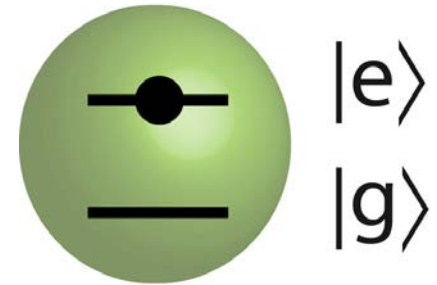
$$g_c \approx \sqrt{Z_0 / R_Q} E_J \approx 1 \text{ GHz}$$



Cooper-pair box = charge qubit

- Small capacitance $E_J / E_C < 1$

$$H_{QB} = -2E_C(1 - 2n_g)\hat{\sigma}_z - \frac{1}{2}E_J\hat{\sigma}_x$$



$$n_g = \frac{C_g V_{dc}}{2e}$$

$$E_C = \frac{e^2}{2C_\Sigma}$$

$$E_J(\Phi_e) = (E_{J1} + E_{J2}) \cos\left(\pi \frac{\Phi_e}{\Phi_0}\right)$$



Cooper-pair box coupled to a phonon

$$H_{QB} = -2E_C(1 - 2n_g)\hat{\sigma}_z - \frac{1}{2}E_J\hat{\sigma}_x$$

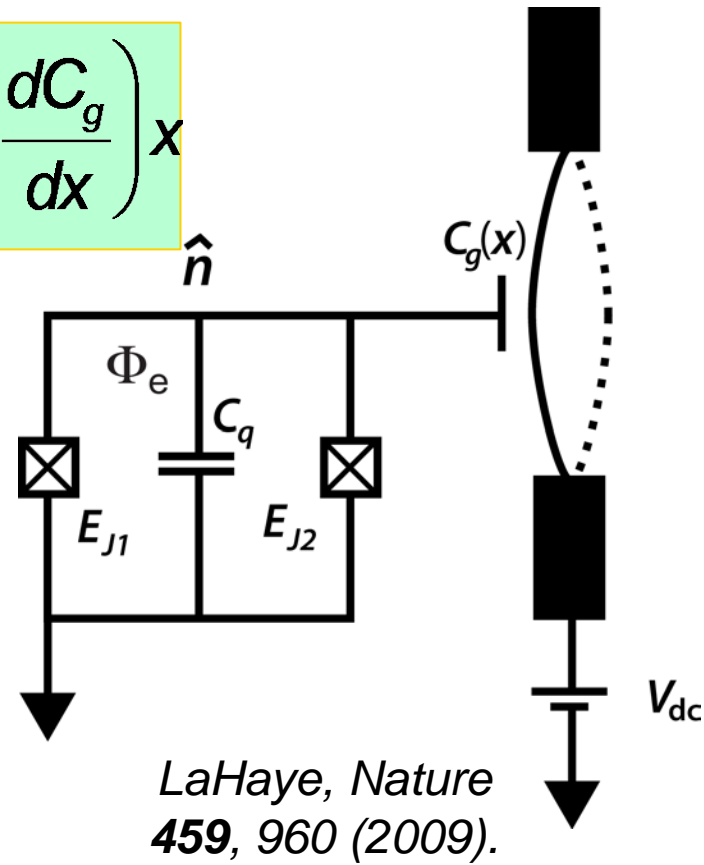
$$C_g(x) = C_{g0} + \frac{dC_g}{dx}x$$

Motion affects
gate charge
(scaled by $2e$)

$$n_g(x) = \frac{V_{dc}}{2e}C_{g0} + \frac{V_{dc}}{2e}\left(\frac{dC_g}{dx}\right)x$$

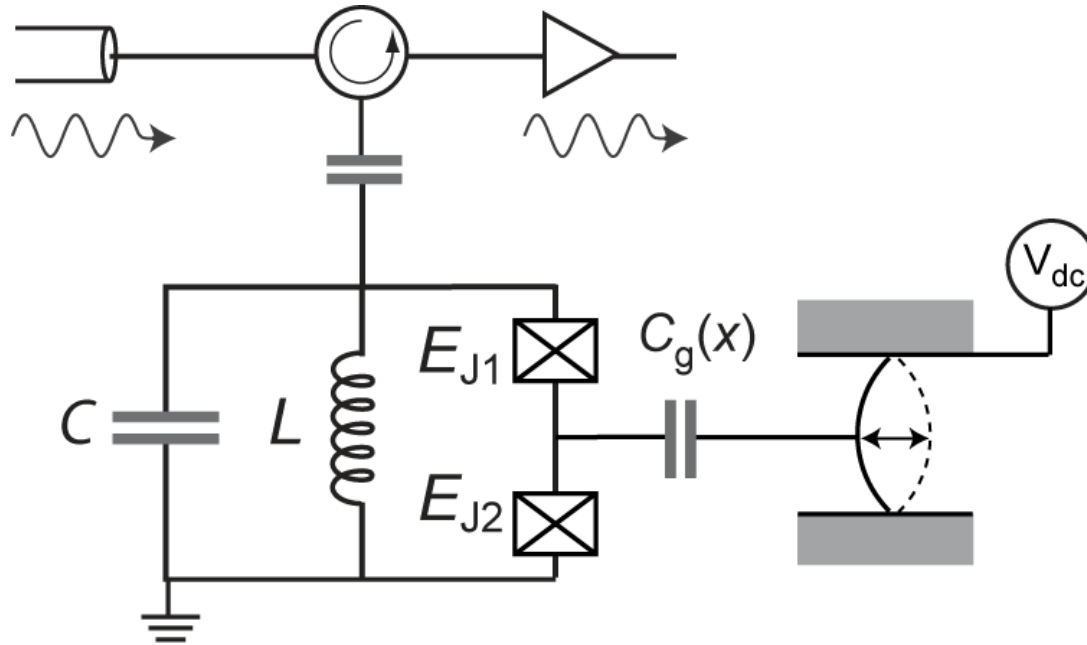
$$\hat{H} = \hat{H}_{QB} + \omega_m\left(\hat{b}^\dagger\hat{b} + \frac{1}{2}\right) - g_m(\hat{b}^\dagger + \hat{b})\hat{\sigma}_z$$

$$g_m = \frac{2E_C}{e}x_{ZP}V_{dc}\left(\frac{\partial C_g}{\partial x}\right) \approx 1 \dots 100 \text{ MHz}$$



Effective optomechanical system

- Qubit-cavity coupling very large



$$H_{\text{QB-c}} = g_c (\hat{a}^+ + \hat{a}) \hat{\sigma}_x$$

$$g_m \approx 100 \text{ MHz} \approx f_m$$

$$H_{\text{QB-m}} = g_m (\hat{b}^+ + \hat{b}) \hat{\sigma}_z$$

$$g_c \approx \sqrt{Z_0/R_Q} E_J \approx 1 \text{ GHz}$$

Effective optomechanical system

- *Qubit tweaks a linear coupling into σ_z coupling*
- Trace out the qubit with Schrieffer-Wolff
- **Effective cavity** couples to **effective** mechanics via **radiation-pressure**

$$H_{\text{eff}} = \omega_c^{\text{eff}} a^\dagger a + \omega_m^{\text{eff}} b^\dagger b + \boxed{g a^\dagger a x} + g_{xx} x_c x + g_4 a^\dagger a b^\dagger b$$

$$\frac{g}{g_0} = \frac{C_g V_{dc} L_{\text{tot}}}{2e} \frac{\partial L_J^{-1}}{\partial n_g} \approx \frac{C_g V_{dc}}{2e} \left(\frac{E_C}{E_J} \right)$$

$$g_{xx} \approx g \ll g_m$$

$$\frac{g_4}{g} \approx \frac{g}{E_J} \frac{R_Q}{Z_0} < 1$$

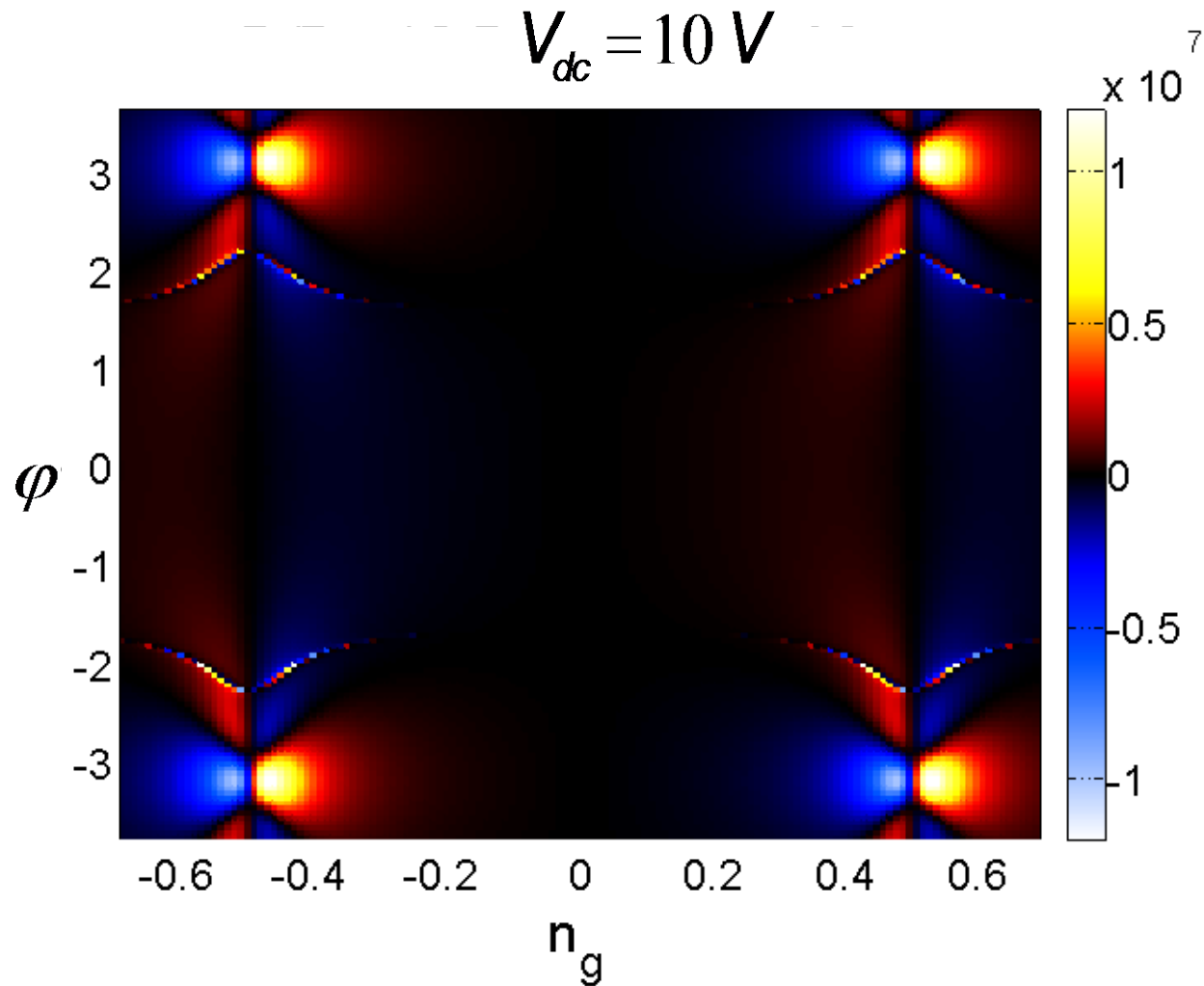
$$V_{dc} = 10 \text{ V}$$

$$E_J/E_C = 0.1$$

$$g/g_0 \sim 10^6$$



Radiation-pressure coupling



Bridge type micromechanical resonator

Al 60 nm

Sapphire

negative PMMA 40...80 nm

Al 300 nm

O₂ plasma

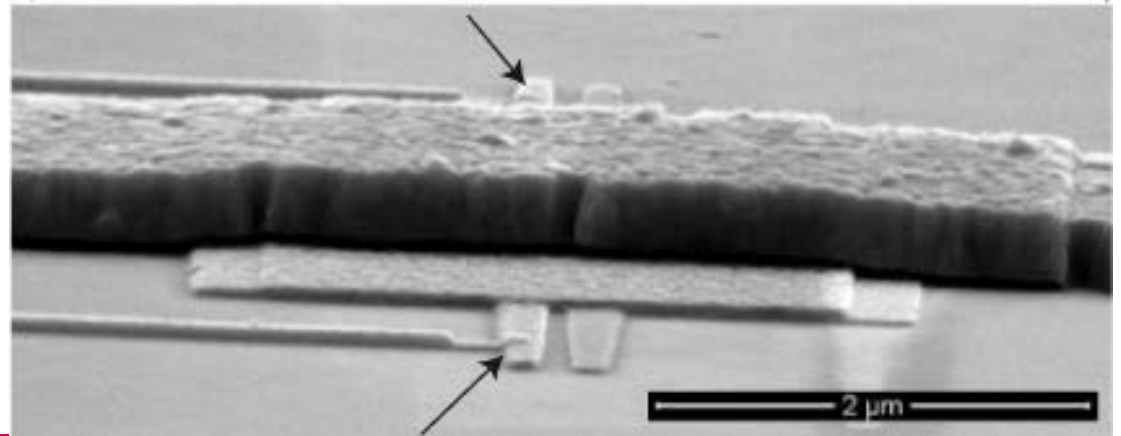
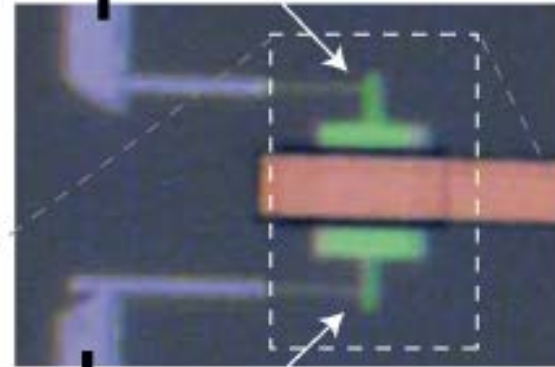
$$L = 5\mu\text{m}$$

$$W = 2\mu\text{m}$$

$$d = 40\text{ nm}$$

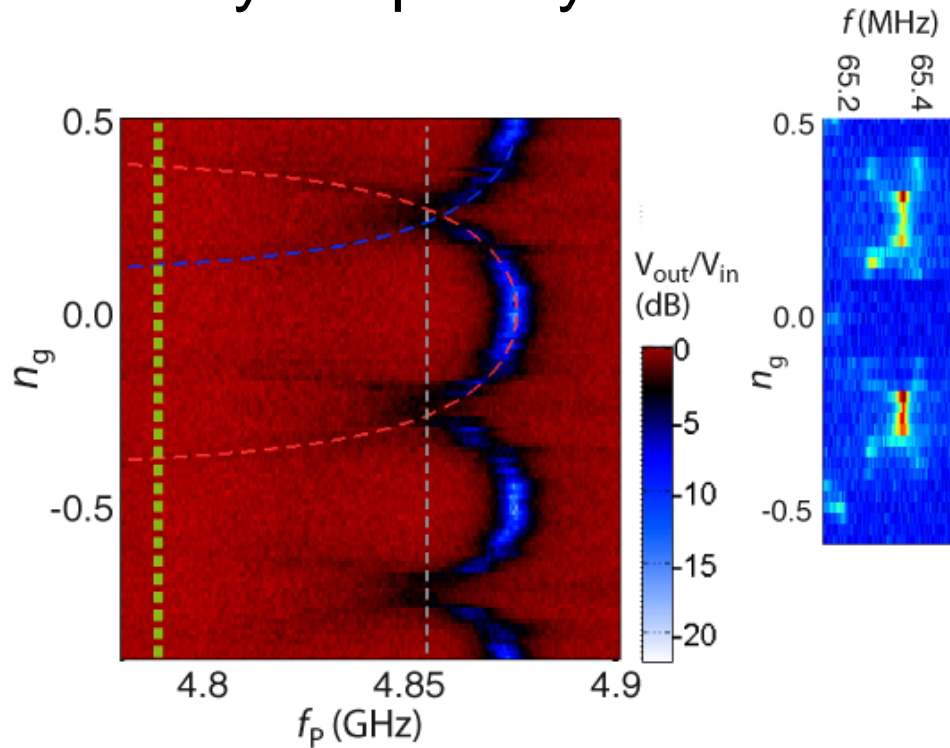
$$x_{ZP} = 6.2\text{ fm}$$

to cavity

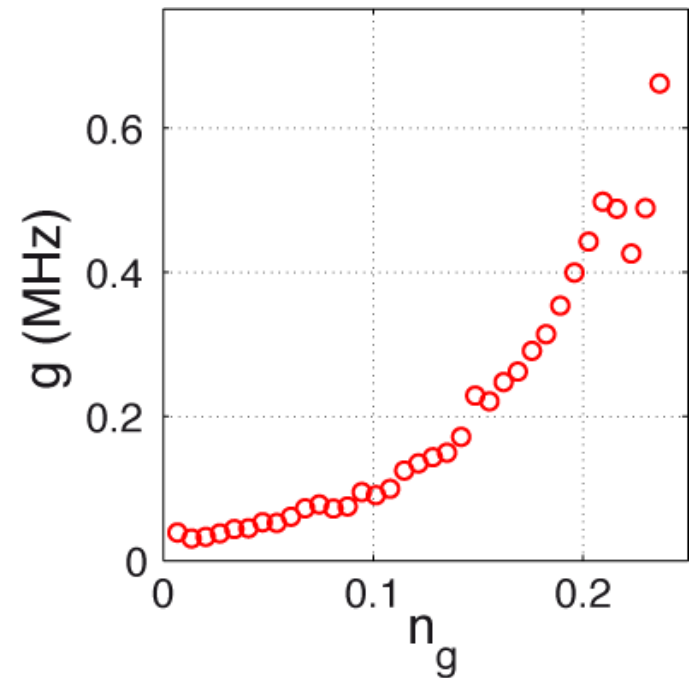


Cavity charge modulation

- Tune down effective $E_J/E_C \rightarrow 0.6$ by flux bias $\Phi_e \approx 0.4\Phi_0$
- Cavity frequency is sensitive to charge



$$V_{dc} = 4.6 \text{ V}$$



$$g \equiv x_{ZP} \frac{\partial f_c}{\partial x} = x_{ZP} \frac{V_{dc}}{2e} \left(\frac{\partial f_c}{\partial n_g} \right) \left(\frac{\partial C_g}{\partial x} \right)$$

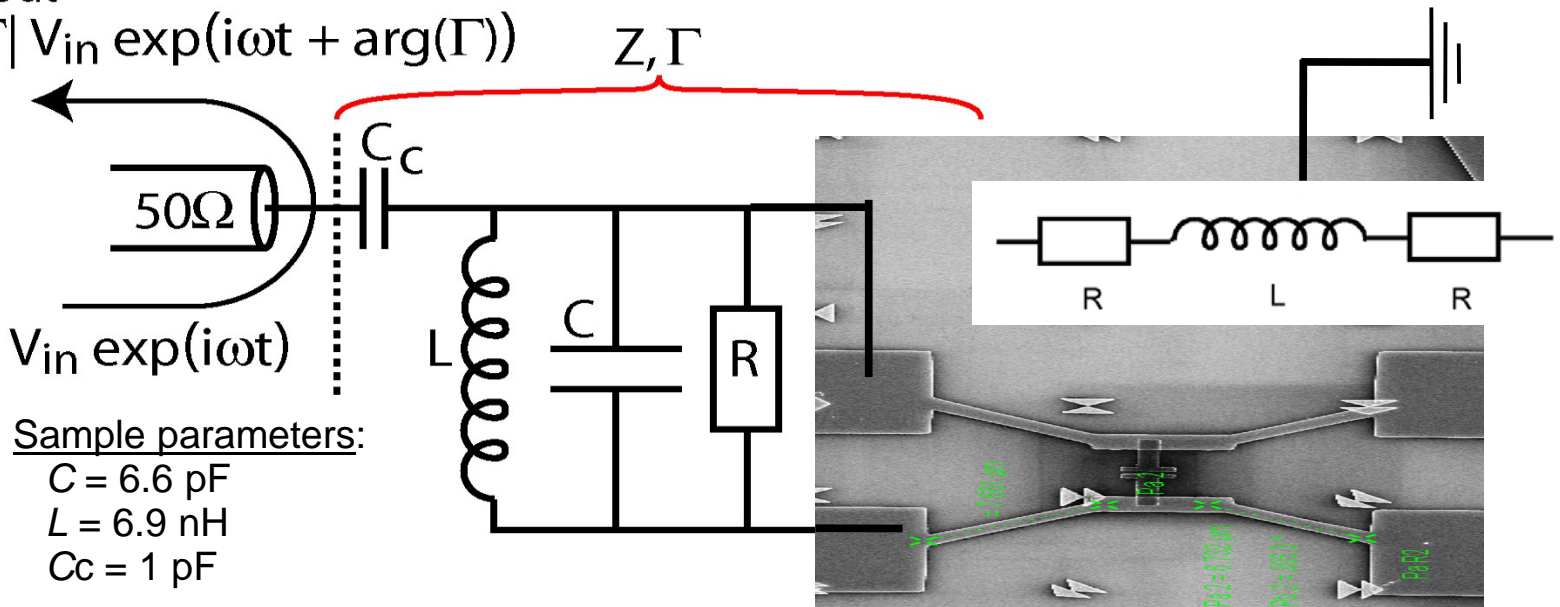
$$1 \text{ Hz} \Rightarrow 0.5 \text{ MHz}$$



Superconducting CNT transistor

$$V_{\text{out}} = |\Gamma| V_{\text{in}} \exp(i\omega t + \arg(\Gamma))$$

Z, Γ



Microwave reflection

$$\Gamma = \frac{Z - Z_0}{Z + Z_0}$$

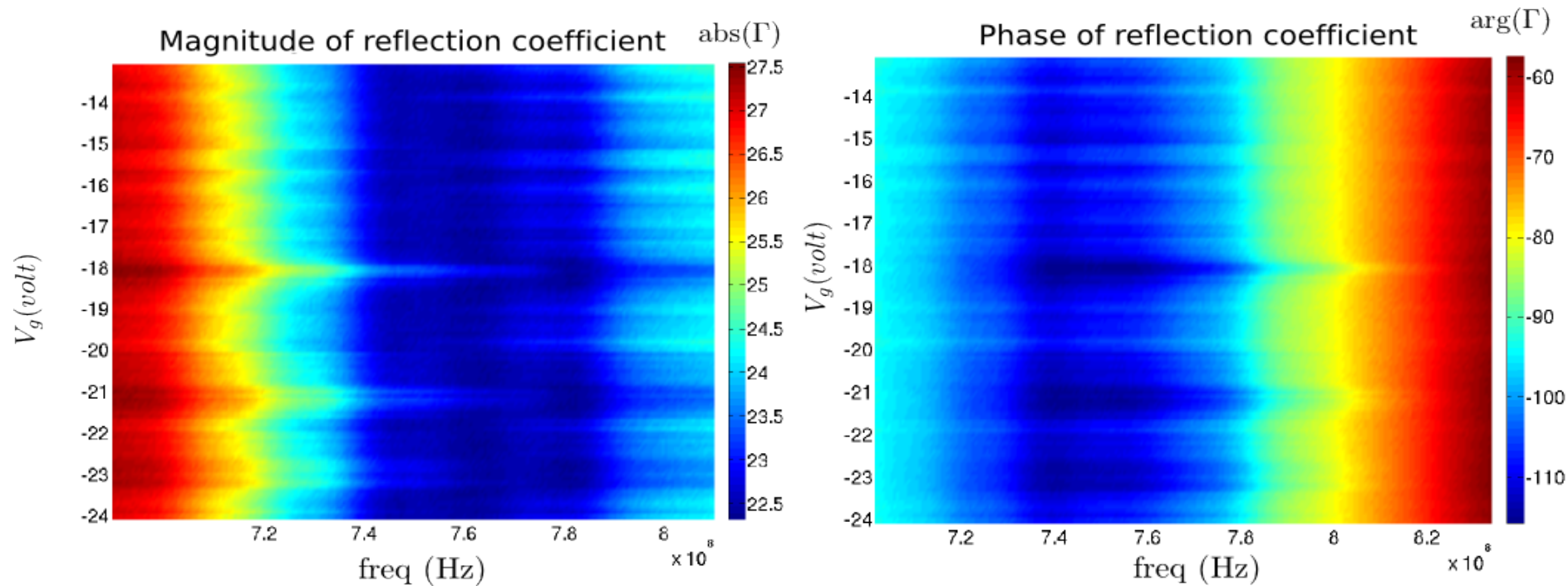
$$Z = \frac{1}{i\omega C_c} + \left(i\omega C + \frac{1}{i\omega L} + \frac{1}{i\omega L_J^*} + \frac{1}{R} \right)^{-1}$$

$$\frac{1}{L} = \left(\frac{2e}{\hbar} \right)^2 \frac{\partial^2 E}{\partial \phi^2}$$

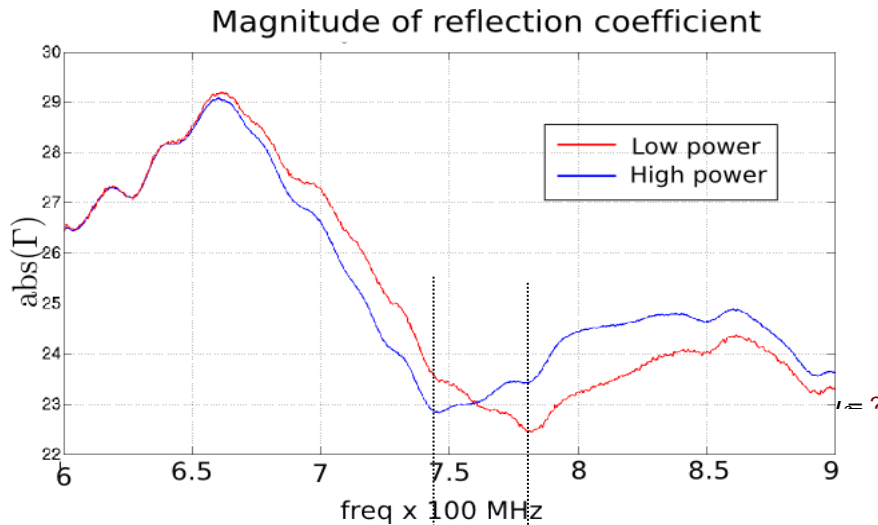
$$L_J = \frac{\hbar}{2eI_C}$$



Gate dependent supercurrent



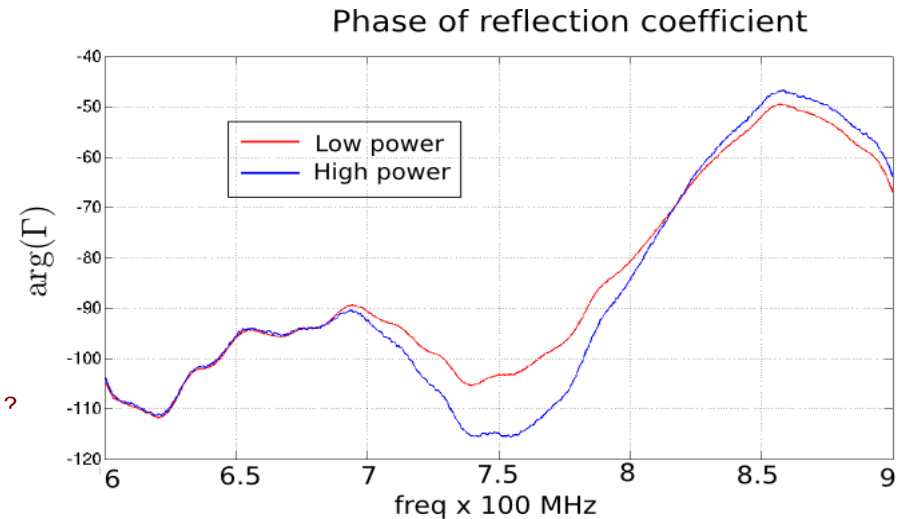
Josephson inductance and supercurrent



$$\Delta f = 37 \text{ MHz}$$

$$\frac{1}{L_j} = C(2\pi f)^2 - \frac{1}{L}$$

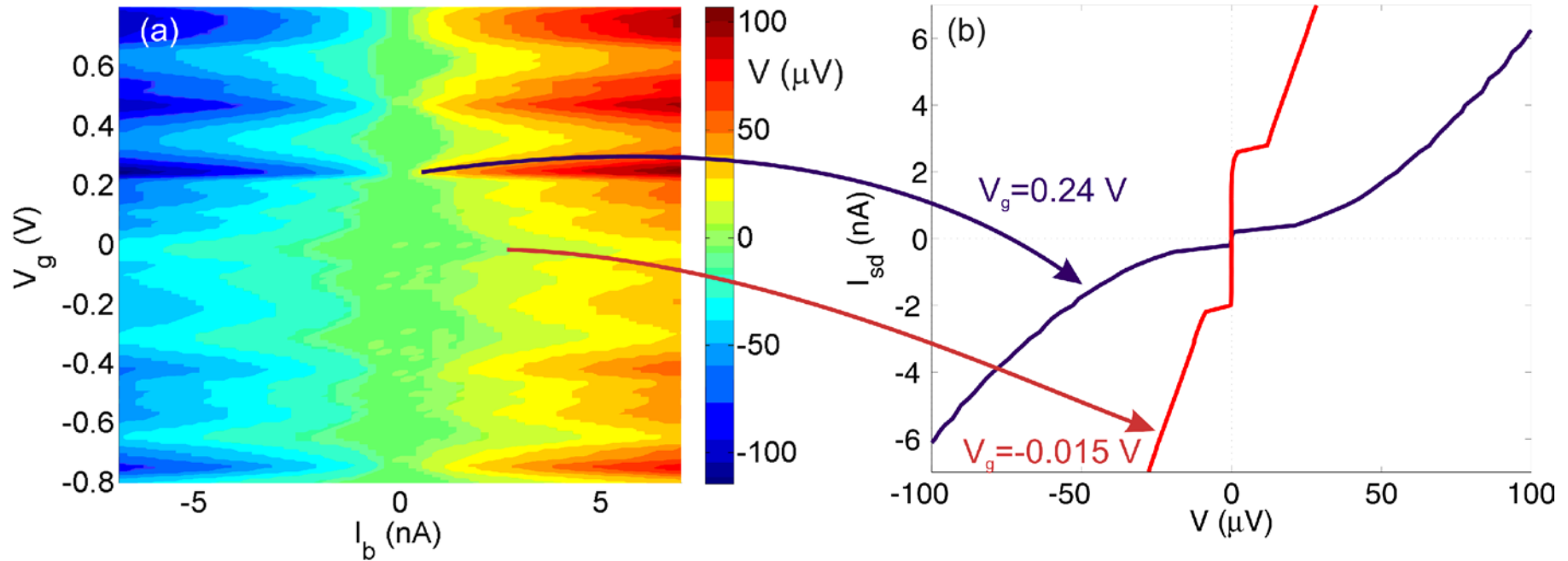
$$I_c = \frac{\hbar}{2eL_J}$$



$$L_J = 68 \text{ nH}$$
$$I_c = 4.8 \text{ nA}$$



I_c modulation and microwaves



P. Häkkinen, A. Fay, P. Lähteenmäki, D. Golubev, and P. Hakonen, APL 2015



Classical phase diffusion

Zero bias resistance:

$$R_0 = \frac{Z_{env}}{I_0(E_J/k_B T)^2 - 1} \quad R_0 = 2Z(0) \left(\frac{k_B T}{E_J} \right)^2$$

Maximum current:

$$E_J \ll k_B T$$

$$I_{cm} = \frac{E_J}{4k_B T} I_{c0} \quad I = \frac{I_{c0}^2}{2} \frac{Z(0)V}{V^2 + \frac{2eZ(0)k_B T}{h}}$$

$$I_{cm} \propto \frac{1}{R_n^2}$$

$$\frac{eV}{k_B T} \ll 1, \quad Z(0) \text{ small}$$

$$I_{cm} \propto I_C^2$$

$$I(V_B) = I_0 \operatorname{Im} \left[\frac{I_{1-2i\beta eV_B/\hbar R_B}(\beta E_J)}{I_{-2i\beta eV_B/\hbar R_B}(\beta E_J)} \right]$$

Yu. Ivanchenko and L. Zil'berman,
Sov. Phys. JETP **28**, 1272 (1969).

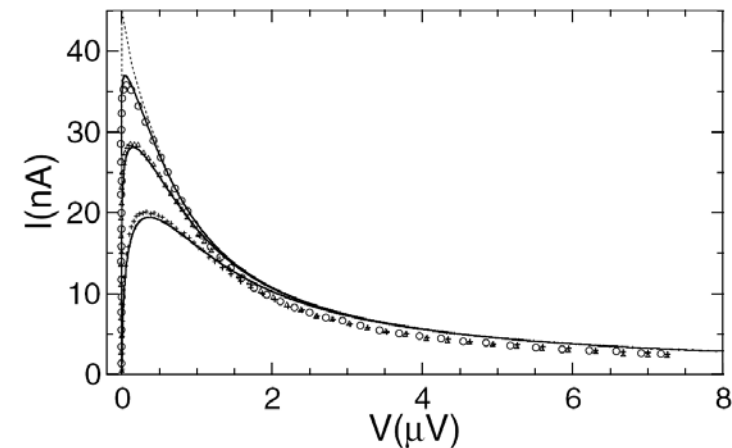


FIG. 3. Comparison between the $I(V)$ characteristics measured at different temperatures (symbols) and the calculated ones (full lines) using Eq. (1) and $I_0 = 44.9$ nA and $R = 24 \Omega$. From top to bottom: $T = 34, 157$, and 400 mK, respectively. Dashed line represents the $I(V)$ predicted at $T = 0$.

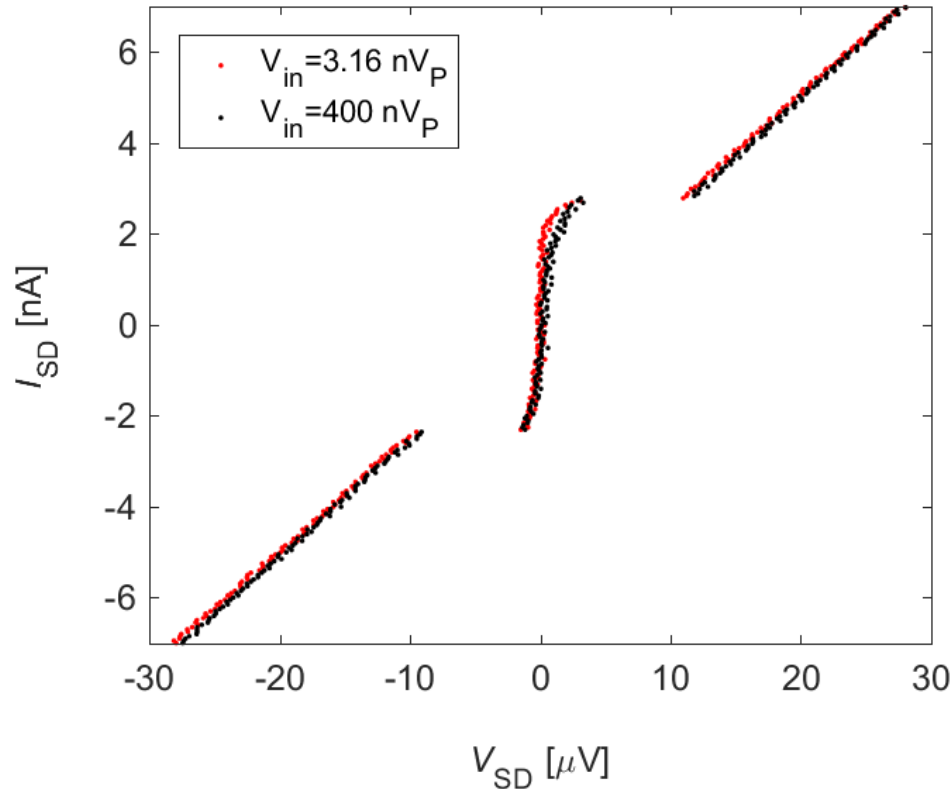
A. Steinbach, et al., Phys.
Rev. Lett. **87**, 137003 (2001).



Maximum of drive amplitude

How high voltage can be applied?

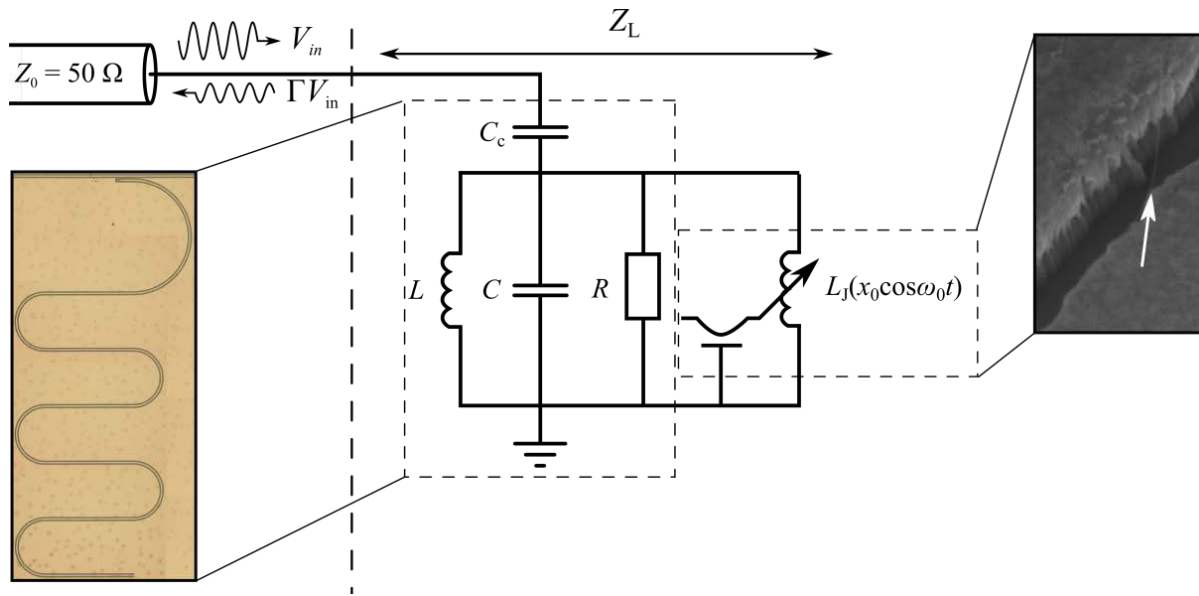
P. Häkkinen, A. Fay, P. Lähteenmäki, D. Golubev, and P. Hakonen, APL 2015



- Experiments with MWNTs suggest that $V_{in} \approx 0.4 \mu V_P$ (-118 dBm) can be applied on source of a $I_{SW} \approx 2.6 \text{ nA}$ junction before the zero voltage branch starts to become resistive.



Coupling to LC-circuit: principle



$$\omega_{\lambda/4} = 2\pi \cdot 5 \text{ GHz}$$

$$L = 2.1 \text{ nH}$$

$$C = 0.49 \text{ pF}$$

$$L_J = 55 \text{ nH}$$

$$\delta L_{J,zpm} = 5 \text{ pH},$$

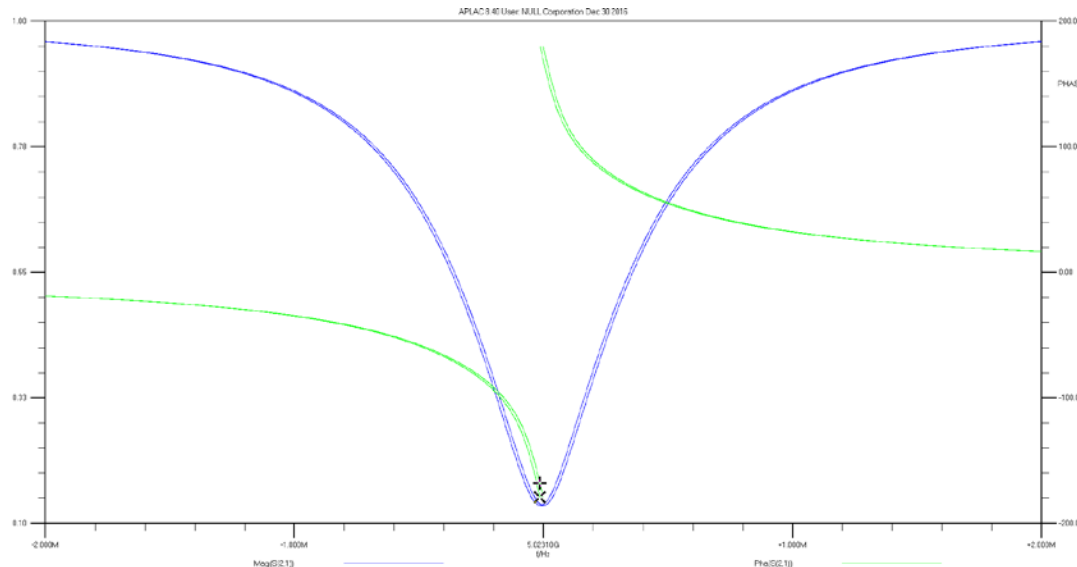
$$\text{when } \delta Q_{G,zpm} = 200 \mu e$$

$$Q_{\text{int}} = 10000$$

$$Q_{\text{ext}} = 17000$$

We would like to know:

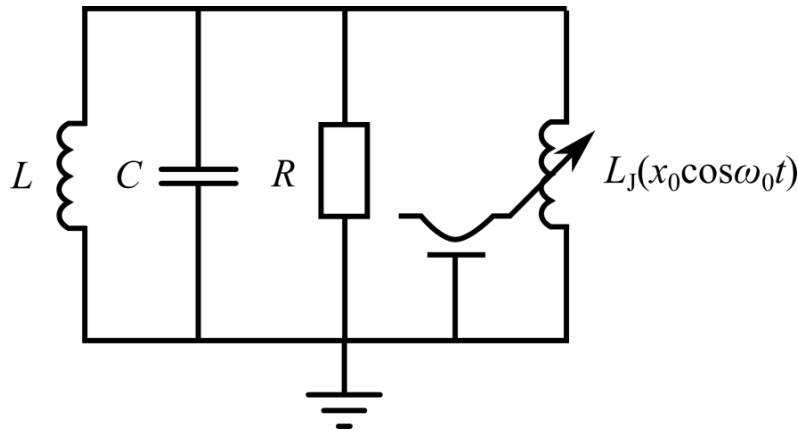
1. Coupling strength
2. Sideband signal to noise ratio



Coupling strength

$$g_0 = \frac{\partial \omega_{0,\text{loaded}}}{\partial x} x_{\text{zpm}} = \frac{\partial \omega_{0,\text{loaded}}}{\partial L_J} \delta L_{J,\text{zpm}}$$

$$\approx \left(1 - \sqrt{\frac{2}{\pi Q_C}} \right) \frac{\partial \omega_0}{\partial L_J} \delta L_{J,\text{zpm}} \approx \frac{\partial \omega_0}{\partial L_J} \delta L_{J,\text{zpm}} \quad \rightarrow \text{OK to neglect coupling capacitor}$$

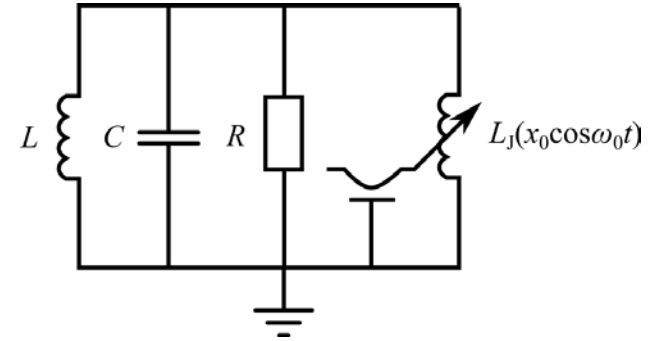
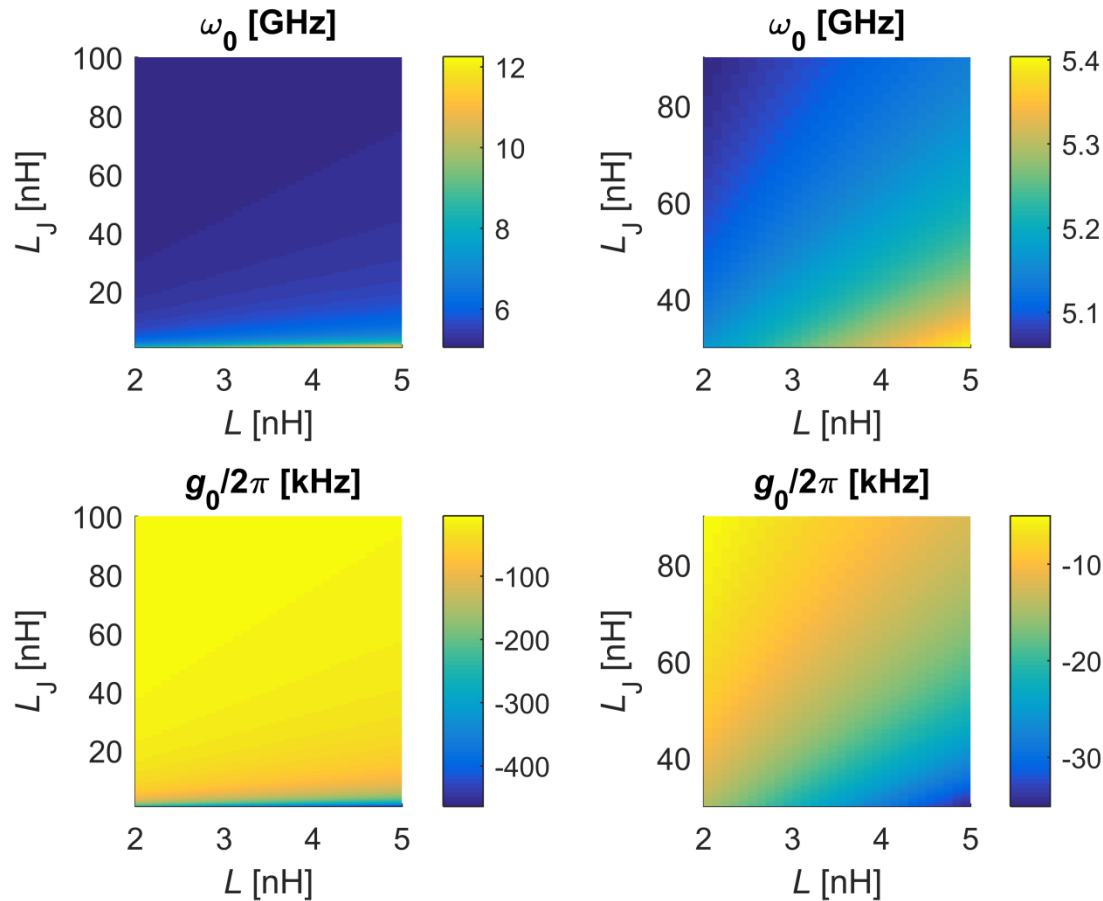


$$\omega_0 = \sqrt{\frac{1}{(L \parallel L_J)C}}, \quad Q_i = \omega_0 RC$$

$$g_0 \approx \frac{\partial \omega_0}{\partial L_J} \delta L_{J,\text{zpm}} = -\frac{\omega_0}{2} \frac{L / L_J}{(L + L_J)} \delta L_{J,\text{zpm}}$$



Coupling strength



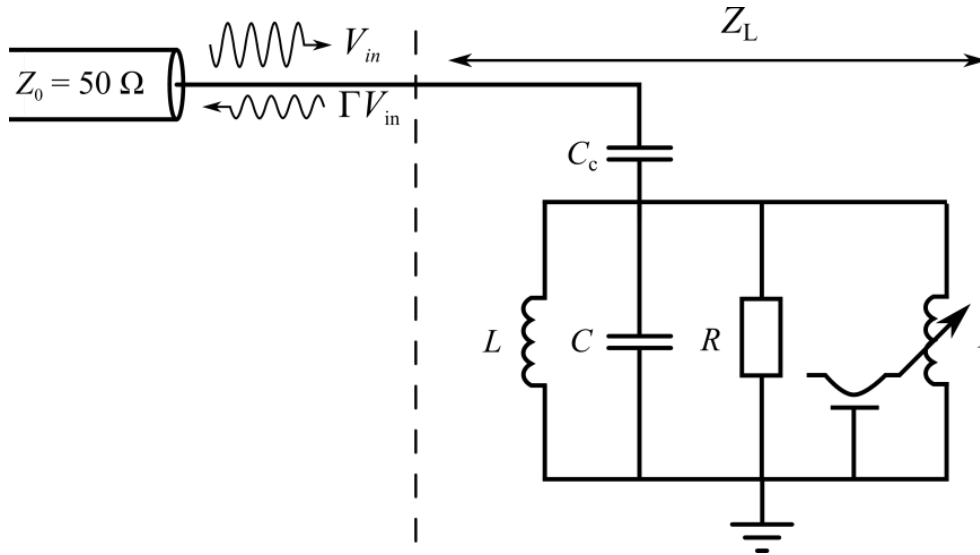
$$\frac{\delta L_{J,\text{zpm}}}{L_J} = \frac{5 \cdot 10^{-12}}{55 \cdot 10^{-9}} \quad \forall L_J$$

$$\omega_{\lambda/4} = 2\pi \cdot 5 \text{ GHz.}$$

$$g_0 = 2\pi \cdot (-8.5 \text{ kHz}) \text{ at } L = 2.1 \text{ nH} \wedge L_J = 55 \text{ nH}$$



Reflection coefficient



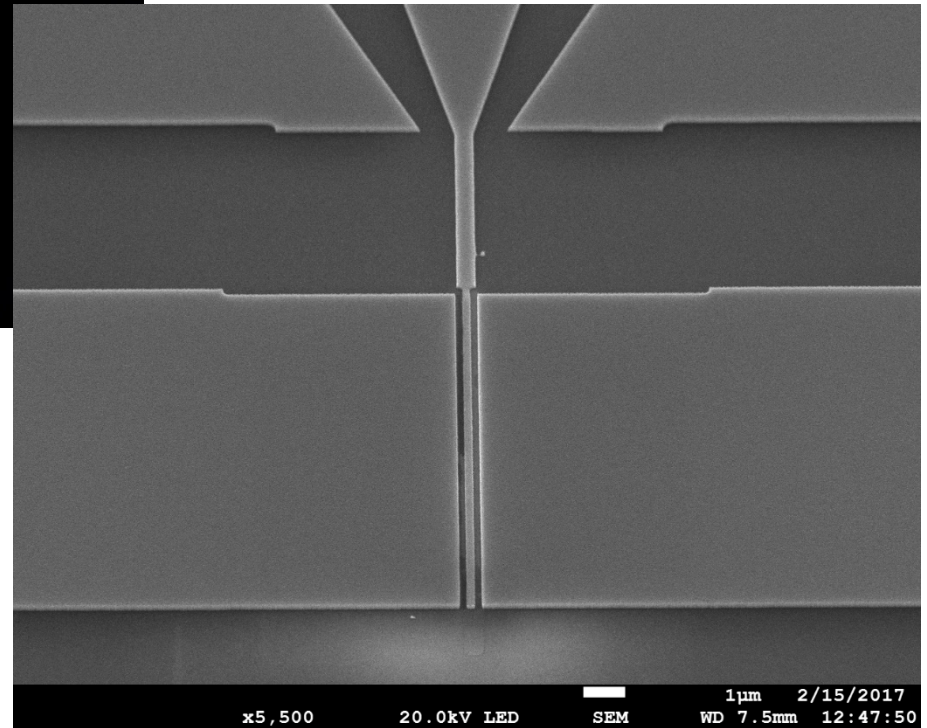
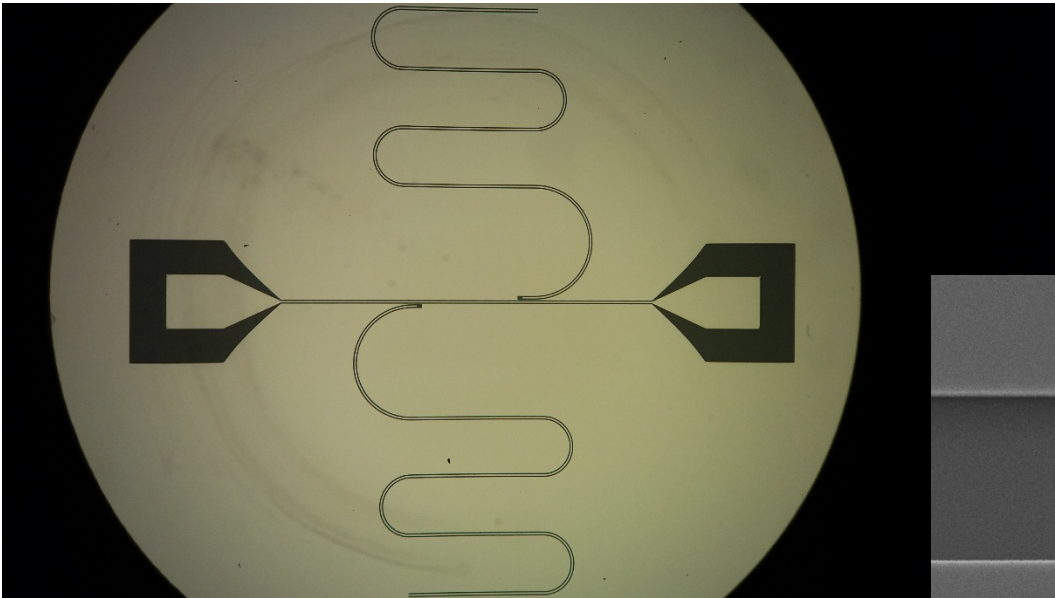
$$\Gamma = \frac{Z_L - Z_0}{Z_L + Z_0}$$

$$\Gamma V_{in} = V_{in} \Gamma|_{\omega_{in}} \cos(\omega_{in} t) + V_{in} \delta \Gamma|_{\omega_{in}} \frac{1}{2} \left\{ \cos[(\omega_{in} + \omega_0)t] + \cos[(\omega_{in} - \omega_0)t] \right\}$$

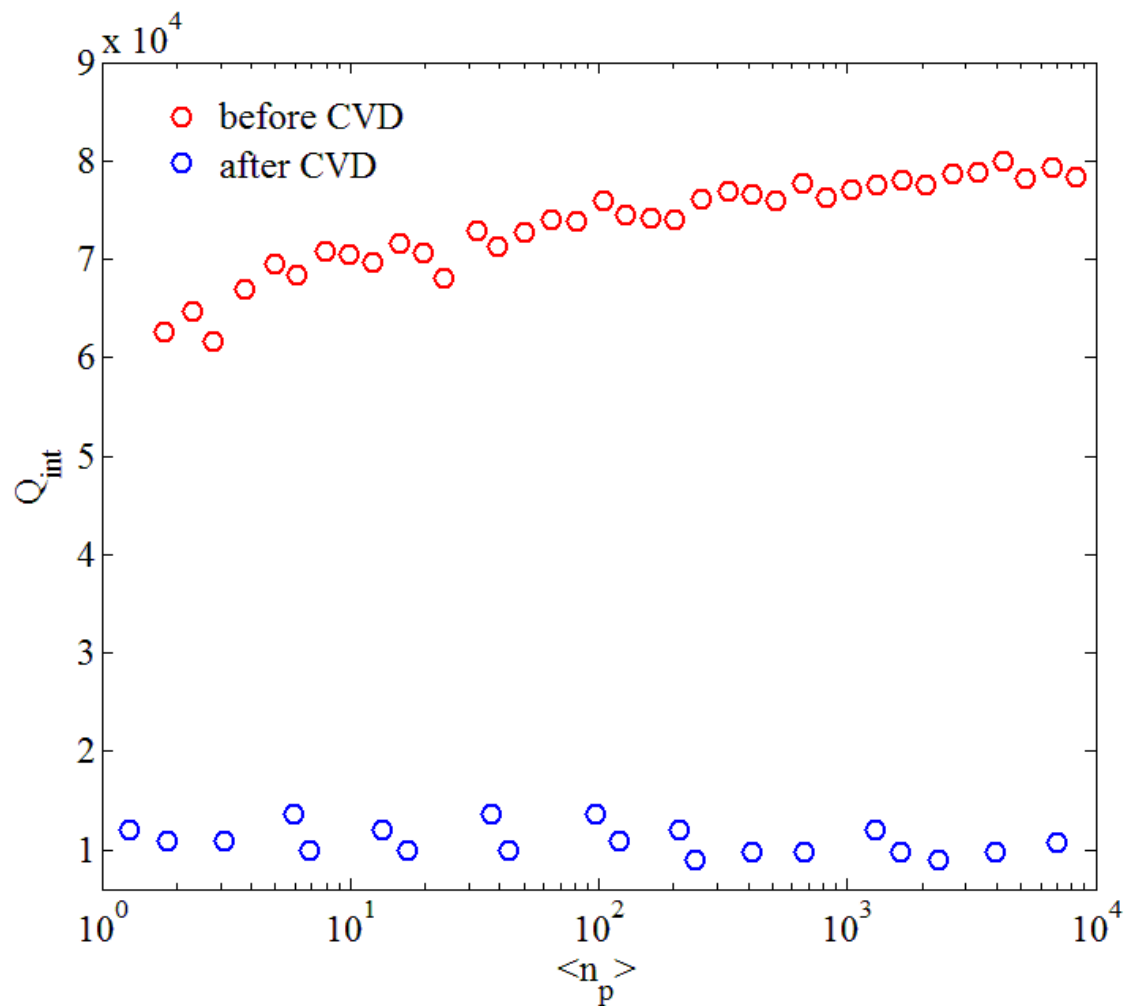
$$\text{Signal: } |V_{\pm}| = \frac{V_{in}}{2} \left| \frac{\partial \Gamma}{\partial x} \right|_{\omega_{in}} x_0 \quad \text{Noise: } \delta V_N = \sqrt{4k_B T_N Z_0 B} \quad SNR = \frac{|V_{\pm}|^2}{\delta V_N^2}$$

$|\delta \Gamma|$ from numerical calculation

MoRe microwave cavity



Losses in microwave cavity



CVD growth of carbon nanotubes

a) Sputter MoRe



b) Deposit 4 Layer Mask



c) EBL, Etch down to Sapphire using RIE, Clean



d) Spin PMMA, EBL, Etch the gate region



e) Spin PMMA, EBL, Deposit catalyst



f) Grow CNT



■ Sapphire

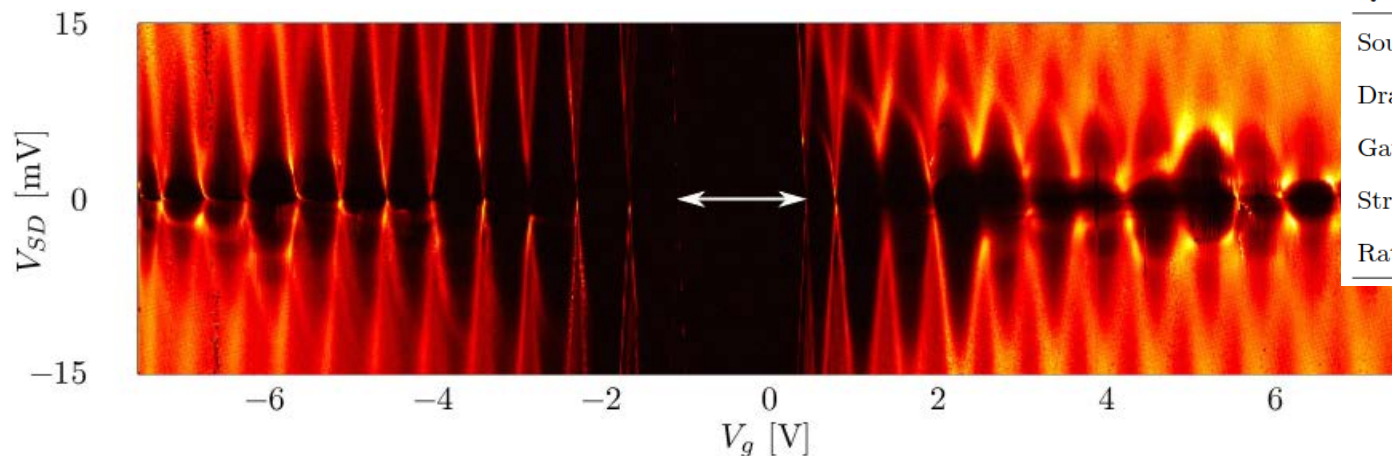
■ MoRe

■ 4 layer Mask
PMMA (125nm)/
Ge (25nm)/
S-1805 (500nm)/
PMMA (125 nm)

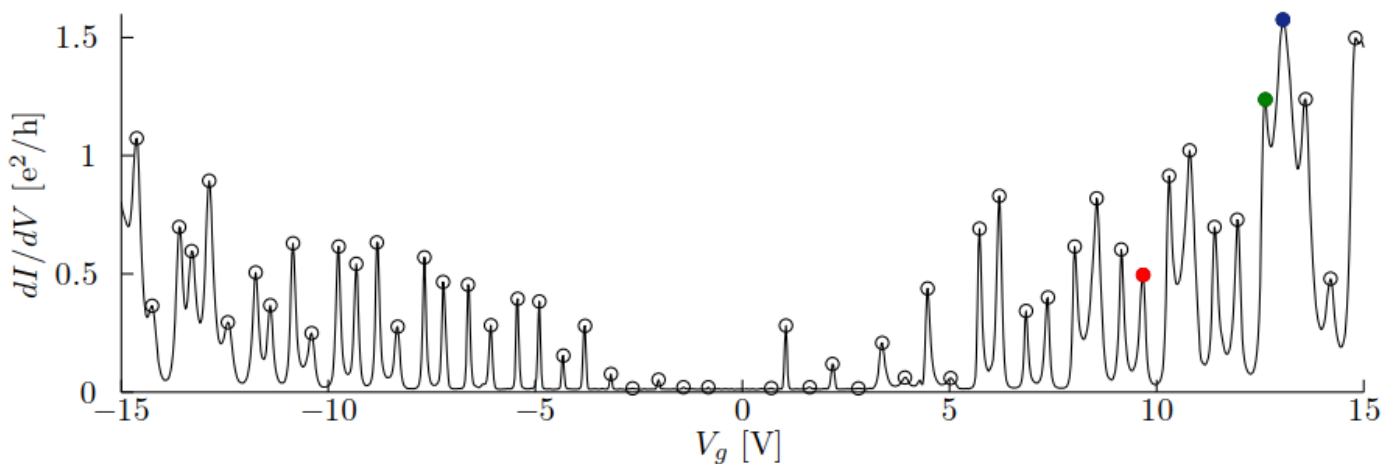
■ Catalyst



Quality of CNTs



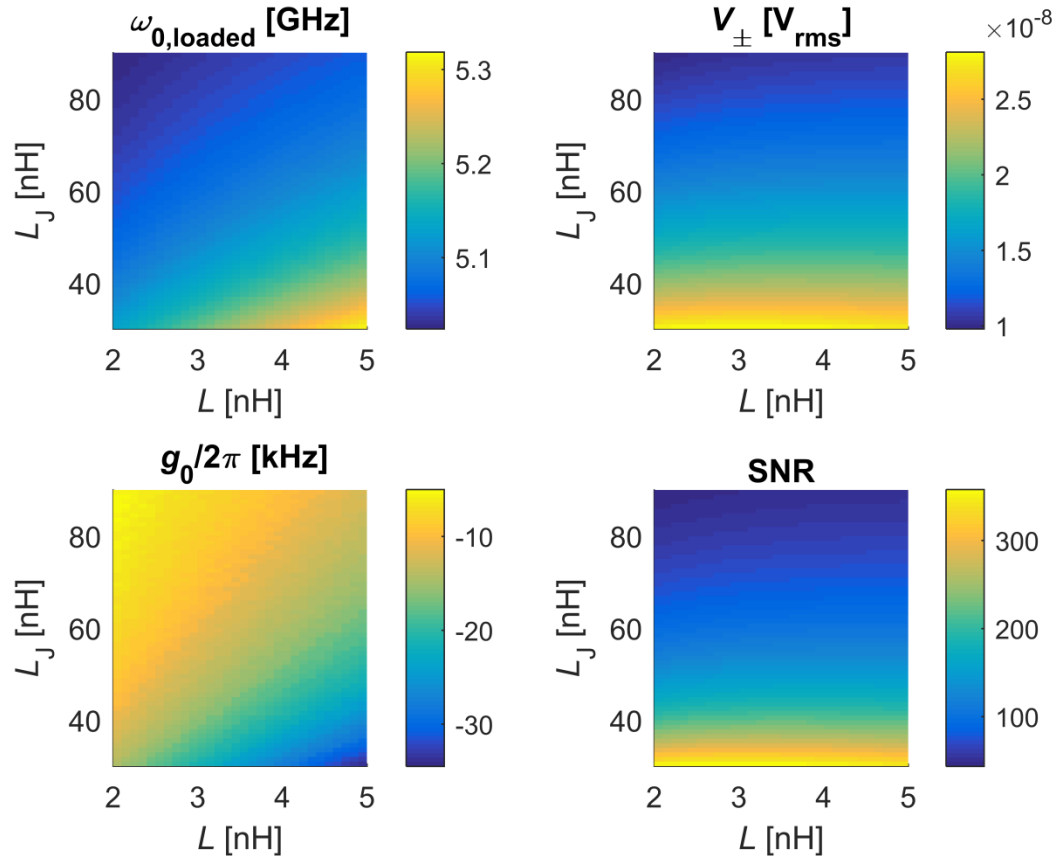
Quantity	Value
Source capacitance, C_S	3.4 aF
Drain capacitance, C_D	7.2 aF
Gate capacitance, C_G	0.34 aF
Stray capacitance, C_0	1.0 aF
Rate constant, $\Gamma_{L,R}/\Delta_D$	$0.25 \times 10^{34} \text{ s}^{-1} \text{ J}^{-1}$



- supercurrents too small

Reflected signal

$$V_{in} = 1 \mu V_P \quad T_N = 4 \text{ K} \quad \text{RBW} = 200 \text{ Hz} \quad Q_{\text{int}} = 10^4 \quad Q_{\text{ext}} = 1.7 \times 10^4$$



$$@ L = 2.1 \text{ nH} \wedge L_J = 55 \text{ nH}$$

$$\omega_0 = 2\pi \cdot 5.085 \text{ GHz}$$

$$g_0 = 2\pi \cdot (-8.5) \text{ kHz}$$

$$V_{\pm} = 15.8 \text{ nV}_{\text{rms}}$$

$$\text{SNR} \approx 113$$

